Optical properties of transition-metal ions in zirconium-based metal fluoride glasses and MgF_2 crystals

Y. Suzuki and W. A. Sibley

Department of Physics, Oklahoma State University, Stillwater, Oklahoma 74078-0444

O. H. El Bayoumi and T. M. Roberts

Rome Air Development Center, Hanscom Air Force Base, Bedford, Massachusetts 01731

B. Bendow

BDM Corporation, 1801 Randolph Road, S.E., Albuquerque, New Mexico 87106

The optical properties of the transition-metal ions, Ni^{2+}, Co^{2+}, and Mn^{2+}, in zirconium-barium-lanthanum-aluminum (ZBLA) fluoride glass are reported. Comparisons of the absorption spectra, luminescence spectra, and luminescence lifetimes for these ions in ZBLA and in MgF_2 crystals have yielded the following results. The crystal field in the glass is much reduced compared with that in MgF_2. The oscillator strengths of the optical transitions for the ions in the glass hosts are almost an order of magnitude larger than similar transitions in MgF_2 crystals, but nonradiative transitions are apparently much more pronounced in the glass. This results in luminescence quenching at lower temperatures in the glass.

I. INTRODUCTION

Heavy-metal fluoride glass (HMFG) has received much attention in recent years because of its potential use as optical fibers and efficient laser hosts,[1-5] and the optical properties of rare-earth ions in HMFG have been widely reported.[6-10] The optical absorption of $3d$-transition-metal ions in HMFG have been intensively investigated to evaluate the transmission losses in infrared transmitting optical light guides,[11-13] and to probe the microscopic structure around $3d$ ions.[14-19] Several investigators[11-19] have discussed the transition energies of $3d$ ions in terms of Tanabe-Sugano diagrams[20] and suggested that $3d$ ions seem to be in O_h-type symmetry in these glasses.

The $3d$ ions have been traditionally important as sensitizers and activators in light-emitting materials. However, there is little data on the optical emission of $3d$ ions in HMFG.[18,19] In this study we evaluate in detail the optical properties of $3d$ ions in zirconium-barium-lanthanum-aluminum (ZBLA) glass ($57ZrF_6$, $36BaF_2$, $3LaF_3$, and $4AlF_3$ in mol %) in order to better understand energy relaxation and oscillator strength values. Both optical absorption and emission were investigated with special emphasis on optical emission. Crystals of MgF_2 were used as a standard host material and the optical absorption and emission for the $3d$ transition-metal ions of Co^{2+}, Ni^{2+}, and Mn^{2+} in glass and in MgF_2 crystals are compared. The optical properties of $3d$ ions in MgF_2 crystals have been widely investigated.[21-34] It has been confirmed that Co, Ni, and Mn ions are substitutional in Mg^{2+} sites and are always divalent. The coordination is that of an orthorhombic distorted F octahedron centered on the cation site of rutile-structured MgF_2 crystals.[22,35] A comparison of the optical properties of these ions in ZBLA glass and MgF_2 provides some "rules of thumb" which are valuable for predicting the usefulness of various materials.

II. EXPERIMENTAL PROCEDURE

ZBLA glasses, of the composition noted earlier and formed with 2 mol % MnF_2 or 0.5, 1.5, and 2.0 mol % CoF_2 or with 0.5 and 1.0 mol % NiF_2 in the melt were prepared at the Rome Air Development Center (RADC). The methods have been described earlier.[36] Crystals of MgF_2 containing 1.6 mol % NiF_2 were furnished courtesy of R. Fahey of Lincoln Laboratory, MIT, while those doped with 0.67 mol % CoF_2 and 1.36 mol % MnF_2 were obtained from Optovac. The concentrations of Mn^{2+} in ZBLA, Co^{2+} in MgF_2, and Mn^{2+} in MgF_2 were determined by EDAX by Professor Z. Al-Shaieb. The concentration of Ni^{2+} in MgF_2 was estimated through a comparison of the measured absorption coefficient with those from samples of known concentration reported previously.[22] The measured concentrations were used to calculate the oscillator strength for the observed transitions. The concentrations of Ni^{2+} and Co^{2+} in the ZBLA melt were employed for the glass calculations.

Low-temperature measurements were made in a liquid-nitrogen cryostat, or a CTI Cryodyne Cryocooler model No. 21SC. The Cryocooler incorporates a resistance heater which allows temperature control within ±2 K over the range 14 to 300 K. For measurements above room temperature samples were enclosed in a copper holder with small windows for the entrance of excitation light and the exit of the fluorescence. A thermocouple was mounted directly on the sample. The temperature was controlled to within ±4 K.

Emission and excitation spectra were taken by exciting the samples with light through a 0.22-m Spex double

monochromator. The fluorescence was focused into a 0.8-m Spex monochromator and detected by either a cooled RCA C-31034 photomultiplier or an optoelectronics OTC-22-53TXXX PbS cell. The photomultiplier signal was preamplified and passed to a lock-in amplifier synchronized with a variable-speed light chopper in the excitation beam. The output of the lock-in amplifier was displayed on an x-y recording or stored by a Hewlett-Packard HP-85 computer. The intensity of the exciting light at the sample position was measured with a Photo-Research Model 310 photometer radiometer. The excitation spectra have been corrected accordingly. The emission spectra have been corrected by calibrating the system with a quartz-iodine lamp traceable to the National Bureau of Standards, U.S. Department of Commerce (Washington, D.C.).

Lifetime measurements were made utilizing a Biomation 610B transient recorder and a Nicholet 1070 signal averager. This system allowed lifetimes as short as 10 μs to be measured. Lifetimes shorter than 10 μs were measured using a Molectron dye laser and a Princeton Applied Research 162 boxcar integrator in the laboratory of R. C. Powell.

Optical absorption measurements were made with a Perkin-Elmer 330 spectrophotometer. Integrated intensities were calculated by numerical integration.

III. EXPERIMENTAL RESULTS

A. Absorption properties

Figures 1 and 2 portray the absorption coefficient of Ni^{2+} and Co^{2+} ions in MgF_2 crystals (upper frames) and in ZBLA glass (lower frames) as a function of wavelength. Figure 3 shows the excitation spectra for Mn^{2+} ions in MgF_2 and ZBLA instead of the absorption spectra, since
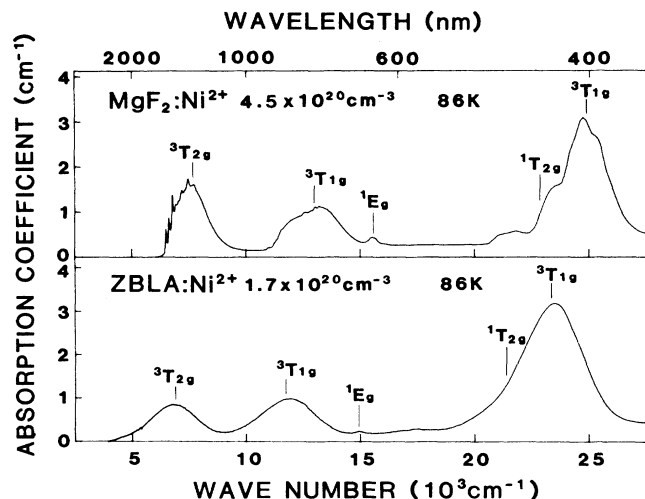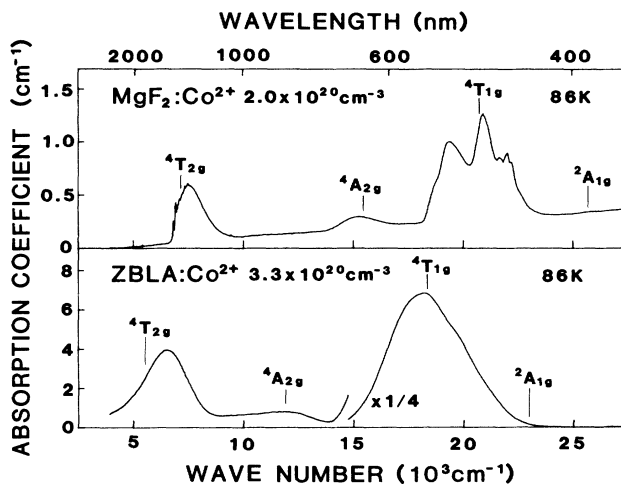

FIG. 2. Unpolarized absorption spectra of Co^{2+} in ZBLA glass and MgF_2 at 86 K. Vertical lines show the calculated transition energies.

the optical absorption was weak. The emission from Mn^{2+} ions was detected at 16 840 cm^{-1} for MgF_2 and at 17 450 cm^{-1} for ZBLA. All spectra were measured at 86 K with unpolarized exciting light. The concentration of the $3d$ ions in MgF_2 crystals and ZBLA glass are presented in the respective frames of Figs. 1 to 3. Although the optical-absorption bands in ZBLA glass are inhomogeneously broadened, which obscures some of the structure, the spectra for both materials are similar. This suggests that the energy-level assignments of the bands for MgF_2 crystals[21-29] are applicable for ZBLA glass.

The observed transition energies and the assignments for the respective $3d$ ions in ZBLA glass and MgF_2 crystals are listed in Table I. The center of gravity for each

FIG. 1. Unpolarized absorption spectra of Ni^{2+} in ZBLA glass and MgF_2 at 86 K. Vertical lines show the calculated transition energies.
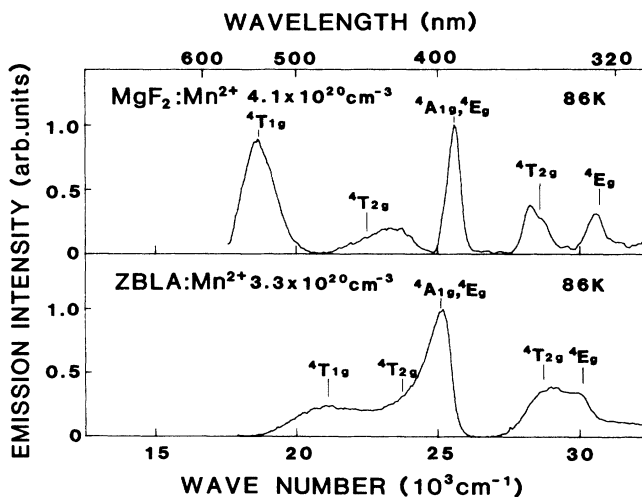

FIG. 3. Unpolarized excitation spectra of Mn^{2+} in ZBLA glass (detected at 17 450 cm^{-1}) and MgF_2 (detected at 16 840 cm^{-1}). Vertical lines show the calculated transition energies.

SUZUKI, SIBLEY, EL BAYOUMI, ROBERTS, AND BENDOW

TABLE I. Absorption properties of Ni^{2+}, Co^{2+}, and Mn^{2+} in ZBLA glass and MgF_2 crystals at 86 K.

| Ion | Assignment | ZBLA glass | | | MgF_2 Crystals | | | f_g/f_c |
		Observed band (cm^{-1})	Calculated peak (cm^{-1})	Oscillator strength f_g	Observed band (cm^{-1})	Calculated peak (cm^{-1})	Oscillator strength f_c	
Ni^{2+}	$^3A_{2g}(F)\text{-}^3T_{2g}(F)$	6780	6900	8.8×10^{-6}	7620	7700	5.0×10^{-6}	1.8
	$\text{-}^3T_{1g}(F)$	11810	11725	11.1×10^{-6}	13020	12999	4.3×10^{-6}	2.6
	$\text{-}^1E_g(D)$	14970	14943	0.1×10^{-6}	15580	15595	0.2×10^{-6}	0.5
	$\text{-}^3T_{1g}(P)$	23360	23375	45.4×10^{-6}	24880	24876	12.2×10^{-6}	3.7
Co^{2+}	$^4T_{1g}(F)\text{-}^4T_{2g}(F)$	6490	5484	24.1×10^{-6}	7660	7187	3.3×10^{-6}	7.3
	$\text{-}^4A_{2g}(F)$	11350	11884	4.6×10^{-6}	15290	15487	0.81×10^{-6}	5.7
	$\text{-}^4T_{1g}(P)$	18380	18368	28.1×10^{-5}	20750	20699	11.5×10^{-6}	24.4
	$\text{-}^2A_{1g}(G)$		22964[a]		25770	25712	0.02×10^{-6}	
Mn^{2+}	$^6A_{1g}(S)\text{-}^4T_{1g}(G)$	21070	21077	1.64×10^{-7}	18690	18670	4.1×10^{-8}	4.0
	$\text{-}^4T_{2g}(G)$	23660	23754	1.13×10^{-7}	23200	22485	1.4×10^{-8}	8.1
	$\text{-}^4A_{1g},^4E_g(G)$	25030	25025	2.79×10^{-7}	25580	25550	2.0×10^{-8}	14.0
	$\text{-}^4T_{2g}(D)$	28740	28674	1.37×10^{-7}	28490	28630	1.2×10^{-8}	11.4
	$\text{-}^4E_g(D)$	29980	30039	1.07×10^{-7}	30670	30660	1.0×10^{-8}	10.7

[a]$C/B = 5.00$ was hypothesized.

absorption band was determined by numerical integration and adopted as the observed transition energy. The overlapping bands for Mn^{2+} in ZBLA were deconvoluted to asymmetric Gaussian bands with the same asymmetries as those for Mn^{2+} in MgF_2. It is notable that all the absorption bands for Ni^{2+} and Co^{2+} occur at lower energies in ZBLA glass than in MgF_2, whereas some absorption bands for Mn^{2+} in ZBLA occur at higher energies with respect to the crystals. The details of these peak shifts

FIG. 4. Integrated absorption coefficients of the 18 380-cm^{-1} band (open circles), the 11 350-cm^{-1} band (open squares), and the 6940-cm^{-1} band (solid circles) of Co^{2+} in ZBLA glass as a function of nominal concentration of Co^{2+} ions.

will be discussed later.

Since glasses containing various concentrations of Co^{2+} were available, it was possible to plot (Fig. 4) the integrated absorption coefficient for the Co^{2+} transitions versus the nominal concentration of Co^{2+} to determine oscillator strengths of the various transitions. The linear relationship suggests only a small loss of Co^{2+} ions in the glass-forming process.

B. Emission properties

The emission from Co^{2+}, Ni^{2+}, and Mn^{2+} in MgF_2 has been reported previously and was duplicated in this experiment.[24-34] The emission transitions of these ions in MgF_2 are shown in the upper panel of Fig. 5. The infrared emission in the figure is not plotted at the same scale. Portrayed in the lower panel is the emission of these ions in ZBLA glass. The emission spectra of Ni^{2+}, Co^{2+}, and Mn^{2+} are represented with solid, dotted, and dashed curves, respectively. The data were taken on the same samples as those used for absorption measurements. The emission spectra and data for Ni^{2+} ions in MgF_2 at 20 K are the same as those reported by Feuerhelm and Sibley.[28] The emission spectra of Ni^{2+} in ZBLA were measured at 15 K. The visible emission was excited at 23 810 cm^{-1}, while the infrared emission was excited by light from 16 700 cm^{-1} to 28 600 cm^{-1} selected by appropriate glass filters. The same exciting light was used to excite Co^{2+} ions in MgF_2 at 15 K. The Co^{2+} emission in ZBLA could not be detected even at 15 K. The emission spectra of Mn^{2+} in MgF_2 and in ZBLA were taken at 86 K with excitation light at 19 230 cm^{-1} and 21 280 cm^{-1}, respectively.

Although the inhomogeneous broadening of the absorption and emission bands in ZBLA is obvious, the correspondence of emission band energies for MgF_2 and ZBLA suggests that the same assignments[24-34] are valid.
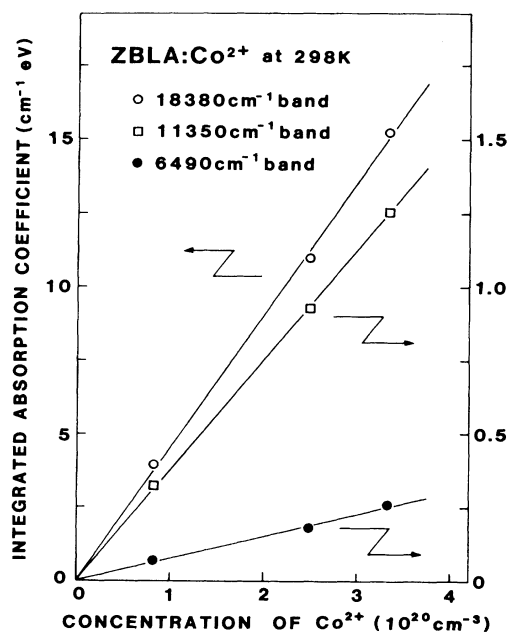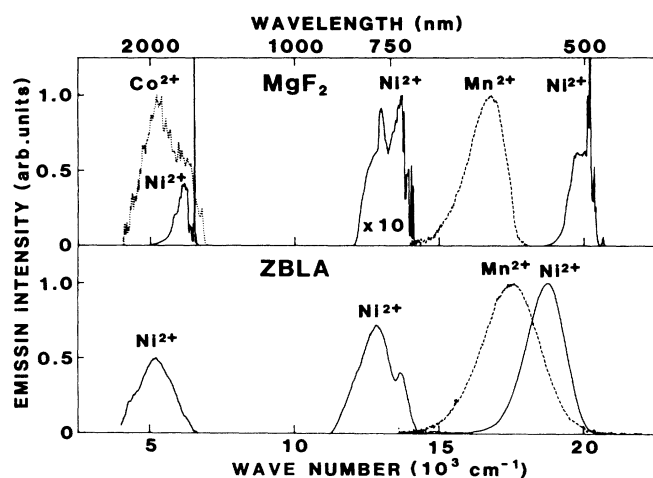
FIG. 5. Emission spectra of Ni^{2+} (solid curves), Co^{2+} (dotted curve), and Mn^{2+} (dashed curves) in ZBLA glass (lower) and MgF_2 crystals (upper). Emission spectra of Ni^{2+} in MgF_2 crystal are from Ref. 28. The relative intensities between the visible and the ir emission for Ni^{2+} are arbitrary.

FIG. 6. Temporal changes of Mn^{2+} emission in ZBLA glass at 86 K (g_1), 298 K (g_2), 472 K (g_3), and MgF_2 at 86 K (c). The emission from ZBLA glass was excited by $21\,410$ cm^{-1} light and detected at $17\,300$ cm^{-1}, for MgF_2 excitation was at $19\,230$ cm^{-1} and emission at $16\,690$ cm^{-1}, respectively.

The level assignments, energies, and half widths of the emission bands observed for the respective ions in ZBLA and MgF_2 are listed in Table II.

Figure 6 shows the emission intensity as a function of time, in milliseconds, for the Mn^{2+} transitions in MgF_2 and in ZBLA. The emission from MgF_2 was excited at $19\,230$ cm^{-1} and detected at $16\,690$ cm^{-1}, while the emission from ZBLA was excited at $21\,410$ cm^{-1} and detected at $17\,300$ cm^{-1}. In the case of MgF_2 at 86 K (curve c) a single exponential decay with a lifetime of 194 ms is observed, whereas in the glass at the same temperature (curve g_1) the emission decay is not single exponential and ranges from 30 to 55 ms. As the temperature increases to 298 K (curve g_2) and 472 K (curve g_3), the emission decay is faster and approaches a single exponential curve. A similar decay profile and temperature dependence was observed for the green emission of Ni^{2+}
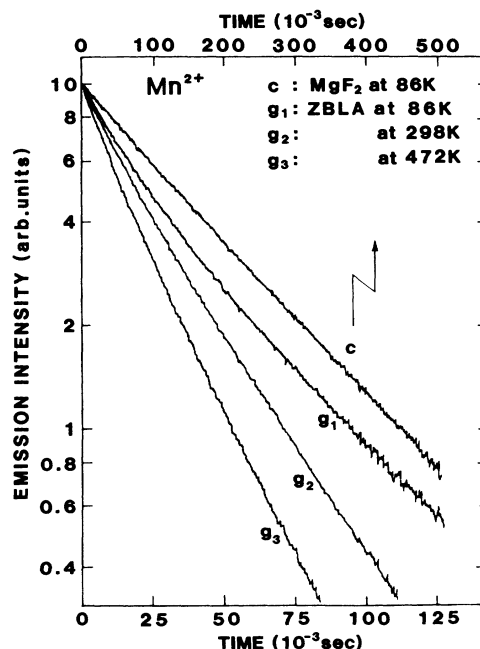
in ZBLA. This is displayed in Fig. 7. The emission was excited at $23\,810$ cm^{-1} and detected at $18\,620$ cm^{-1}. The deviation from a single exponential decay is prominent at 11 K.

Figures 8—10 illustrate the temperature dependence of the lifetimes (solid symbols) and the integrated intensities (open symbols) of the emission. In the case of glass, the lifetimes were obtained from the slope at the times when the intensities reached 40% of the initial intensity. The lifetimes of Mn^{2+} emission are plotted in Fig. 8. In both ZBLA (solid triangles) and MgF_2 (solid circles) the life-

TABLE II. Emission properties of Ni^{2+}, Co^{2+}, and Mn^{2+} in ZBLA glass and MgF_2 crystals.

Ion	Assignment	ZBLA glass Band (cm^{-1})	Half width (cm^{-1})	Lifetime[a] (s)	MgF_2 crystals Band (cm^{-1})	Half width[b] (cm^{-1})	Lifetime (s)
Ni^{2+} (15 K)[c]	$^3T_{2g}(F)$-$^3A_{2g}(F)$	5200	1460	3.7×10^{-4}	5880	420	1.3×10^{-2}
	$^1T_{2g}(D)$-$^3T_{2g}(F)$	12 840	1540		13 200	1420	3.9×10^{-4}
	$^1T_{2g}(D)$-$^3A_{2g}(F)$	18 660	1540	3.2×10^{-6}	19 940	850	4.0×10^{-4}
Co^{2+} (15 K)	$^4T_{2g}(F)$-$^4T_{1g}(F)$	d			5430	1790	1.60×10^{-3}
Mn^{2+} (86 K)	$^4T_{1g}(G)$-$^6A_{1g}(S)$	17 480	2330	4.4×10^{-2}	16 580	1500	1.9×10^{-1}

[a]From the decay slope at 40% of the initial intensity. The decay profile was not single exponential.
[b]The phonon spike was neglected.
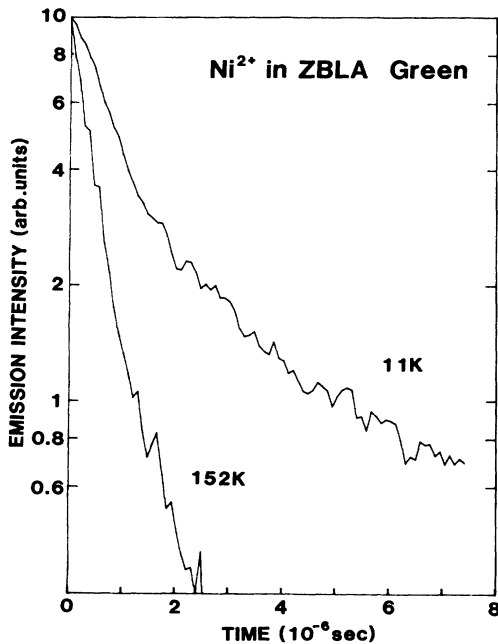[c]Data of MgF_2 are from Ref. 26 (20 K).
[d]Undetectable.

FIG. 7. Temporal change of the green emission from Ni^{2+} in ZBLA glass at 11 and 152 K. The emission was excited by 23 810 cm^{-1} light and detected at 18 620 cm^{-1}.
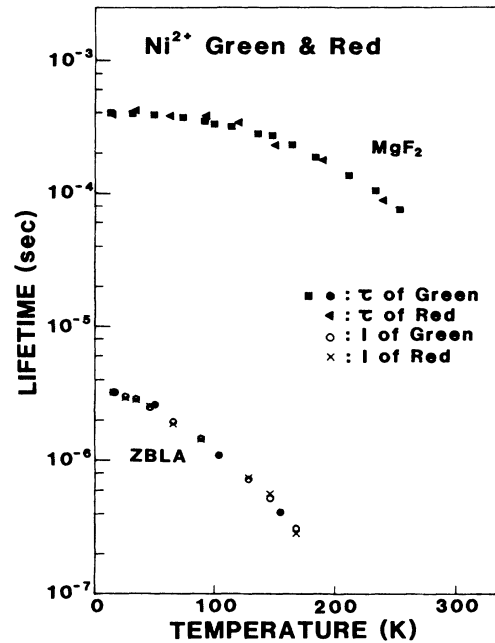
FIG. 9. Temperature dependence of the lifetime of the green emission from Ni^{2+} in ZBLA glass (solid circles); the green (solid squares) and the red emission (solid triangles) from Ni^{2+} in MgF$_2$ crystals (Ref. 28). Temperature dependence of the integrated intensities of the green and the red emission from ZBLA glass are shown by open circles and crosses, respectively. The photon energies for excitation and detection are provided in the text.
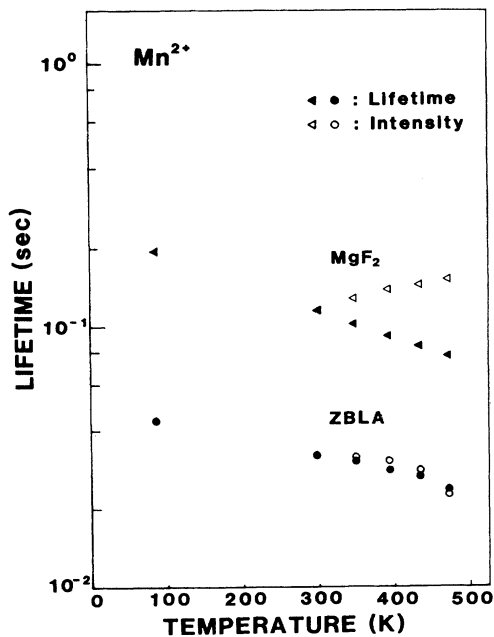
FIG. 8. Temperature dependence of the lifetimes (solid symbols) and integrated intensities (open symbols) of Mn^{2+} emission in ZBLA glass (circles) and MgF$_2$ crystals (triangles). The photon energies for excitation and detection are provided in the text.

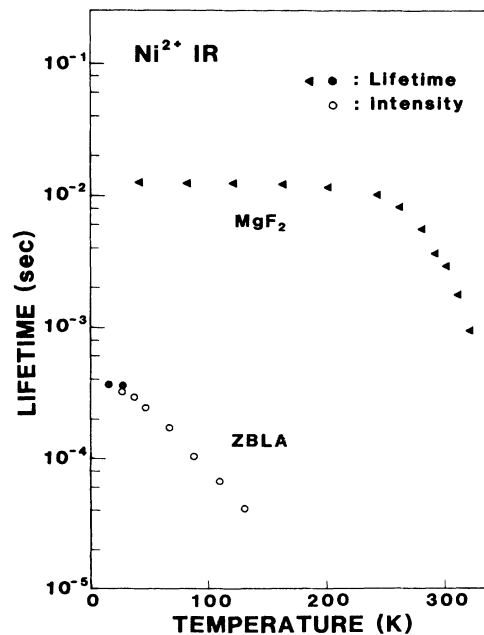FIG. 10. Temperature dependence of the lifetimes of Ni^{2+} ir emission from ZBLA glass (solid circles) and MgF$_2$ crystals (solid triangles) (Ref. 28). The integrated intensities of Ni^{2+} ir emission from ZBLA glass are shown by open circles.

times gradually decrease with increasing temperature. The lifetimes for ZBLA are much shorter at all temperatures than those for MgF_2. The integrated intensities above 300 K are given in Fig. 8. Since the integrated intensities are on the arbitrary scale, they are normalized to the lifetimes at 300 K. The Mn^{2+} intensities in ZBLA (open circles) follow the change of the lifetimes, whereas those in MgF_2 (open triangles) do not. These results imply that the temperature dependences of the lifetimes in ZBLA and MgF_2 are dominated by different mechanisms in spite of the apparent similar behavior.

The lifetimes of the visible emission from Ni^{2+} are portrayed in Fig. 9.[28] The agreement for the green (solid squares) and the red emission (solid triangels) provide further evidence for the transition assignments.[24] In ZBLA only the green emission decay was measured. The lifetimes obtained are plotted as solid circles. Notice that the lifetimes in ZBLA are much shorter than for MgF_2. The open circles and crosses represent the intensities of the green and red emission and they are normalized to the lifetimes at 15 K. Clearly, the assignments for the Ni^{2+} transitions in MgF_2 are also applicable for ZBLA. The similarity of the temperature dependence of the lifetimes and intensities suggests that the lifetime decrease of the visible emission in ZBLA is due to thermal quenching. This process is much more effective in ZBLA than in MgF_2. Figure 10 provides data on the lifetimes and intensities of the ir emission from the Ni^{2+} ion. The response time of the PbS cell is around 200 μs and precluded data at high temperatures. The integrated emission intensities (open circles) are normalized to the lifetime value at 15 K. As in the case of the visible emission, the infrared emission from ZBLA:Ni^{2+} is quenched at a much lower temperature than in MgF_2 and the lifetimes are much shorter. The lifetimes are listed in Table II.

FIG. 12. Tanabe-Sugano diagram for Co^{2+} (Ref. 20). Vertical dotted lines show the normalized crystal field in ZBLA glass and MgF_2 crystals at 86 K.

IV. DISCUSSION

A. Transition energies of $3d$ ions in glass

The details of the site symmetry around $3d$ ions and $3d$-F distances in glass are not well known. It varies from ion to ion so the "crystal field" fluctuates. Nevertheless,

FIG. 11. Tanabe-Sugano diagram for Ni^{2+} (Ref. 20). Vertical dotted lines show the normalized crystal field in ZBLA glass and MgF_2 crystals at 86 K.

FIG. 13. Tanabe-Sugano diagram for Mn^{2+} (Ref. 20). Vertical dotted lines show the normalized crystal field in ZBLA glass and MgF_2 crystals at 86 K.

TABLE III. Crystal-field and Racah parameters for Ni^{2+}, Co^{2+}, and Mn^{2+} in ZBLA glass and MgF$_2$ crystals at 86 K. The accuracies of Dq, B, and C/B are ± 2.5 cm^{-1}, ± 2.5 cm^{-1}, and ± 0.035, respectively, except for those for ZBLA:Co^{2+}.

Parameter	Ion		
	Ni^{2+}	Co^{2+}	Mn^{2+}
Dq for ZBLA (Dq for MgF$_2$) (cm^{-1})	690 (770)	640 (830)	630 (955)
B for ZBLA (B for MgF$_2$) (cm^{-1})	960 (985)	920 (975)	715 (730)
C/B for ZBLA (C/B for MgF$_2$)	4.20 (4.30)	(5.00)	5.00 (5.00)

the peak shifts between the absorption bands in ZBLA and MgF$_2$ (Figs. 1—3) can be explained by utilizing the Tanabe-Sugano diagrams for octahedral symmetry field (Figs. 11—13). The crystal-field parameter Dq and the Racah parameters B and C were determined by the method of least squares from the observed transition energies in Table I, and are listed in Table III. The transition energies estimated from the crystal-field parameters are represented by the vertical lines in Figs. 1—3 and are listed in Table I. The normalized crystal fields Dq/B in ZBLA glass and in MgF$_2$ crystals are depicted by the dotted vertical lines in Figs. 11—13. The crystal field is considerably less for the glass. The energy of the emission bands for 3d ions in ZBLA are shifted from those in MgF$_2$ (Fig. 5). This can be understood from the lower crystal field in ZBLA. In the case of Mn^{2+} ions, the decrease of the crystal field results in a blue shift of the emission band in ZBLA from that in MgF$_2$ (Fig. 5).

In the ZBLA emission spectra for Ni^{2+} ions, a prominent red shift of the infrared band and green band, and a slight red shift for the red band compared to MgF$_2$ spectra, are observed. As shown in Fig. 11, the decrease of the crystal field results in the reduction of the transition energies from $^3T_{2g}$ to $^3A_{2g}$ (ir band), and from $^1T_{2g}(D)$ to $^3A_{2g}$ (green band), but the red emission originates from the transition from $^1T_{2g}(D)$ to $^3T_{2g}$. In this case the energy curves of these levels are almost parallel so that a change of the crystal field does not result in a significant change in the transition energy between these levels.

B. Environment of 3d ions

The crystal field and Racah parameters for 3d ions in zirconium fluoride glass are listed in Table IV. The variation of Dq values accurately follows the ordering of the spectrochemical series,
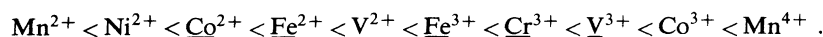
$$\underline{Mn}^{2+} < Ni^{2+} \leq \underline{Co}^{2+} < \underline{Fe}^{2+} < V^{2+} < \underline{Fe}^{3+} < \underline{Cr}^{3+} < \underline{V}^{3+} < Co^{3+} < Mn^{4+} .$$

TABLE IV. Crystal field and Racah parameters for 3d ions in zirconium fluoride glass.

Ion[a]	Dq (cm^{-1})	B (cm^{-1})	C (cm^{-1})	Host	Reference
Mn^{2+}	630	715	3575	ZBLA (86 K)	present
Fe^{2+}	893			ZBLANaPb	13
Co^{2+}	744	820		ZBGdANa	11
	764	858		ZBLANaPb	13
	640	920		ZBLA (86 K)	present
Ni^{2+}	663	956	4006	ZBGdANa	11
	654	1045		ZBLANaPb	13
	690	970		ZBLA	19
	690	960	4600	ZBLA (86 K)	present
Cu^{2+}	1031			ZBLANaPb	13
Ti^{3+}	1923			ZBLANaPb	13
V^{3+}	1498	716		ZThB	14
	1536	658		ZBGdA	11
	1536	665		ZBLANaPb	13
Cr^{3+}	1468	845		ZThB	14
	1475	847	3136	ZBGdA	11
	1471	816		ZBLANaPb	13
	1480	850		ZBLA	19
Fe^{3+}	1239	1163	2870	ZBGdA	11

[a]All except for Cu^{2+} (T_d) are O_h symmetry.

This series was proposed by Jorgensen as an empirical law for the ordering of the crystal field for octahedral ligands in liquid phase.[37] Although the large increase of Dq values for trivalent ions can be understood from an increased Coulomb interaction, the observed ordering for ions with the same valence state is still not well understood. However, it is evident that the ions in ZBLA glass act as if they were in a liquid phase because of the more open glass structure.

On the other hand, as seen in Table III, the variation of Dq values for $3d$ ions in MgF$_2$ crystal does not follow the spectrochemical series. This is not unexpected since Dq is theoretically inversely proportional to the fifth power of the internuclear distance between the central ion and the surrounding ligands.[38] In MgF$_2$ crystals, the ligand distance is primarily restricted by the lattice constant. However, the ionic radii of $3d$ ions (Ni^{2+}:0.69 Å, Co^{2+}:0.75 Å, and Mn^{2+}:0.83 Å) are considerably larger than the Mg^{2+} ion (0.65 Å). When they replace Mg^{2+} ions a strong crystal-field effect occurs due to the effective decrease in ligand distance. The ratio of the averaged internuclear distances in MgF$_2$ crystals (a_c) to those in ZBLA glass (a_g) can be estimated according to the following relation:

$$a_c/a_g = (Dq_g/Dq_c)^{1/5} .\qquad(1)$$

In this case Dq_g and Dq_c are the glass and MgF$_2$ crystal fields, respectively. The calculated results show that the Ni—F, Co—F, and Mn—F bond lengths in MgF$_2$ are 98%, 95%, and 92%, respectively, of the lengths in ZBLA glass. This is consistent with the ionic radii of the respective ions, and explains the relatively large change of the crystal field for Mn^{2+} from crystal to glass.

It is tempting to use the optical properties of $3d$ ions as a probe to investigate local structure[15] but care must be exercised. Several models have been suggested for the microscopic structure of fluorozirionate glass.[39–41] In all models, Ba^{2+} ions for which the $3d$ impurities probably substitute are taken as network modifiers. However, the excellent agreement of the data with the Tanabe-Sugano diagrams and the small inhomogeneous broadening of the spectra suggest that the crystal field at Ba^{2+} ion sites can be approximated by deformed octahedral ligands. This is not the normal situation for network modifiers. Network modifiers usually occupy sites with a variety of coordination numbers and crystal-field strengths. In fact, the x-ray data of Coupe et al.[42] indicate coordinate numbers for Ba^{2+} ranging from 8.70 to 10.68. The decrease in Racah parameter B in ZBLA from that in MgF$_2$, suggests, either an increase of the bond covalency or a decrease of the coordination number.[43] The ionic radius of the Ba^{2+} ion (1.36 Å) is larger than those of the $3d$ ions, and the $3d$ ions may not sit at the Be^{2+} site center. Recently, White et al.[44,45] proposed that some $3d$ ions partially distort the local structure to accommodate their own bonding requirements in glasses. They form "metal-ligand complexes." In such a case, the optical spectra of $3d$ ions would not directly reflect the long-range structure around $3d$ ions but that of a local arrangement. This concept would explain the present results satisfactorily. This behavior can be rationalized as due to the high ionicity of the ZBLA glass but further investigation is required.

C. Oscillator strengths of $3d$ ions in glass

Oscillator strengths for each transition in ZBLA glass and MgF$_2$ crystals were estimated from the Smakula equation[46] [Eq. (1)] and are presented in Table I as f_g and f_c, respectively,

$$f = \frac{0.821\times10^{17}}{N}\frac{n}{(n^2+2)^2}\int \alpha(E)dE .\qquad(2)$$

The dopant concentrations N are listed in the figures. The refractive indexes n for ZBLA and MgF$_2$ were provided by Drexhage et al.[47] and Duncanson et al.,[48] respectively. The integrated absorption coefficients $\int \alpha(E)dE$ were computed numerically. Since the absorption of Mn^{2+} in MgF$_2$ could not be detected, the oscillator strength for $^4A_{1g}$, ^4E_g in KMgF$_3$:Mn^{2+} at 1.7 K reported by Ferguson et al.[49] was utilized for the normalization. The relative intensities of each transition for Mn^{2+} in MgF$_2$ are rather different from those in KMgF$_2$, and the absolute values of the oscillator strengths for Mn^{2+} in MgF$_2$ could be in error by a factor 3. It should be noted that in all three transition-metal ions the oscillator strengths in ZBLA glass (f_g) are larger than those in MgF$_2$ (f_c), except for the $^3A_{2g} \to {}^1E_g$ transition in Ni^{2+}. The ratio of the oscillator strengths between ZBLA glass and MgF$_2$ crystals is listed in the last column of Table I.

The $3d$ ion optical properties are mainly due to electric dipole transitions although these transitions are strictly forbidden by Laporte's selection rule: $\Delta l = \pm1$, in the free-atom. The actual oscillator strength is determined by the degree of the relaxation of this parity selection rule.[38] Two mechanisms were proposed by Van Vleck[50] for removal of the forbiddeness. One is the absence of inversion symmetry and the other is a distortion of the inversion symmetry by odd-mode thermal vibrations. For the centrosymmetric $3d$ ion complex with symmetry O_h only the latter process is effective. Consequently, the oscillator strengths are low ($10^{-7}–10^{-6}$) and are sensitive to temperature.[43] For noncentrosymmetric complexes, the former process is predominant and results in relative high ($10^{-6}–10^{-4}$) spin-allowed oscillator strengths relatively insensitive to temperature.[43] Thus the temperature dependence of the oscillator strengths allows a distinction to be made between the two processes and provides further information on the site symmetry of $3d$ ions in glass. Our temperature dependence measurements show an 80% increase in absorption coefficient for Co^{2+} in MgF$_2$, as the temperature increases from 86 to 298 K, whereas in ZBLA:Co^{2+} only a 7% increase is observed. This result strongly suggests that the enhancement of the oscillator strengths for ZBLA are induced by static distortions of the normally octahedral ligands.

It is worthwhile to point out the similarity between the present spectra and those on the $3d$ complexes with no inversion symmetry. Wood et al.[51] compared the absorption spectra of Cr^{3+} ions in K$_2$NaCrF$_6$ (O_h symmetry) and those in emerald (no center of symmetry). The overall spectra for emerald were essentially analogous to those for K$_2$NaCrF$_6$, but the absorption intensity was 10 times higher than for K$_2$NaCrF$_6$.

Borromei et al.[52] investigated Ni^{2+} and Co^{2+} spectra in MWO_4 (M=Mg,Zn,Cd) crystals. Both the Ni^{2+} and Co^{2+} ions have C_{2v} site symmetries in these host lattices. They found two interesting effects: (1) large enhancement of the absorption intensities for the transitions at higher energies and (2) the absorption intensities for the $^4T_{1g}(F) \rightarrow ^4T_{1g}(P)$ transition of Co^{2+} ions were drastically enhanced. This behavior is remarkably similar to the present results on the oscillator strengths in ZBLA glass listed as f_g/f_c in Table I. Borromei et al.[52] interpreted their first result in terms of the mixing of the $3d$ electrons and the p electrons of the ligand oxygens. The mixing is most effective for the higher excited states of the $3d$ ions. Their second finding was attributed to an enhanced dipole transition between the ground and excited states induced by a distorted charge distribution. They suggested that transitions between the ground and the excited states with the same symmetries are especially intense. This same explanation could apply to $3d$ ions in ZBLA.

D. The branching ratio of Ni^{2+} visible emission

Although the emission spectra of Ni^{2+} ions in ZBLA and MgF_2 are similar (Fig. 9), the branching ratio of the red emission to the green emission in ZBLA is much enhanced. The red and the green Ni^{2+} emissions are attributed to transitions from $^1T_{2g}(D)$ to $^3T_{2g}(F)$ and $^3A_{2g}$, respectively.[26-28] Thus, the explanation for the selective enhancement of absorption intensities discussed in the preceding section is applicable.[52] The identical symmetry of the initial and the final state can result in a relative enhancement of the red emission intensity. However, the $^1T_{2g}(D)$ states are mixed with the $^3T_{1g}(D)$ states through spin-orbit interaction,[26-28] and the actual transition probabilities are dominated by the contribution of the $^3T_{1g}(D)$ term so the spin-orbit interaction must be considered.[53]

E. Thermal quenching of the emission in ZBLA glass

Figures 8–10 illustrate that the temperature dependence of the emission is much more prominent in glass than in MgF_2. This strong temperature dependence could arise from energy transfer or from multiphonon transitions between electronic levels. The temperature dependence of the energy transfer rate is dominated by the spectral overlap between absorption and emission.[54] Because of inhomogeneous broadening, the spectral overlap is larger in a glass than in a crystal. Thus, energy transfer is generally enhanced in glassy materials. However, the transfer rate is relatively insensitive to higher temperatures in glass. For example, the half width of the ir absorption band for Ni^{2+} in ZBLA glass increased only 8% when the temperature increased from 86 to 298 K. This change is too small to explain the drastic decrease of the lifetimes and intensities of the ir emission.

The strong thermal quenching of the emission is most likely attributed to multiphonon emission processes. The probability of a multiphonon transition is proportional to the square of the following matrix element:[55]

$$v(mr \rightarrow ns) = \sum_k J^k(m,n) F^k(mr,ns) , \qquad (3)$$

where $J^k(m,n)$ is the electronic term:

$$J^k(m,n) = \left\langle \phi_m^0 \left| \frac{\partial He}{\partial Q_k} \right| \phi_n^0 \right\rangle . \qquad (4)$$

In this case ϕ^0 is an electronic function and Q_k is the vibration coordinate. $F^k(mr,ns)$ is a vibrational factor, which is the product of a promoting term and an overlap factor of the accepting mode. From this factor a classical Arrhenius form is obtained in the strong-coupling limit, and an energy-gap law can be deduced for the weak-coupling limit.[56] Although the energy-gap law has been widely utilized for the evaluation of the multiphonon emission processes for rare-earth ions,[57-59] it is not appropriate for $3d$ ions. The multiphonon emission rate for ir emission from Ni^{2+} in MgF_2 at 250 K can be estimated from Fig. 10 as 30 s^{-1}. This value is 2 orders smaller than that for the Co^{2+} emission reported by Moulton (6×10^3 s^{-1}),[29] in spite of their almost identical energy separation from the ground state. For the integral in Eq. (4) to be nonzero, the normal modes of the local vibration around impurity ions must contain the same representation as the direct product of the initial and final electronic wave functions.[55,60-63] Robbins and Thompson[55] examined the selection rules for transition-metal ions in O_h and T_d symmetry. They found that for internal conversion from $^3T_{2g}$ to $^3A_{2g}$ for Ni^{2+} ions with O_h symmetry there is no promoting mode in the normal modes of vibration, whereas E_g and T_{2g} vibrations act as promoting modes to trigger the $^4T_{2g} \rightarrow ^4T_{1g}(F)$ transition in Co^{2+} with O_h symmetry. Consequently the multiphonon emission rate in a Co^{2+} system can be more enhanced compared with that for Ni^{2+}.

This point of view has been invoked by Andrews et al. to explain the small quantum efficiencies of Cr^{3+} emission in a variety of glassy materials.[62,63] When this selection is relaxed through distortion of the symmetry of ligands in glass, more effective thermal quenching occurs. For example, if C_{4V} symmetry is assumed instead of O_h, the level $^3T_{2g}$ in Ni^{2+} splits to $^3B_2 + ^3E$ and conversion from $^3A_{2g}$ to $^3B_1$ allows a normal-mode E vibration to act as the promoting mode for internal conversion which results in low-temperature quenching.

The absence of Co^{2+} emission in ZBLA glass can also be understood from this viewpoint. The E_g and T_{2g} vibration modes are available for the promotion of $^4T_{2g} \rightarrow ^4T_{1g}(F)$ transition in O_h symmetry; however, for C_{4v} symmetry, all the normal modes (A_1, B_1, B_2, E) can contribute to the internal conversion from $B_2 + E$ to $A_2 + E$. This results in a significant quenching of the emission.

F. Emission lifetimes for ZBLA glass

The lifetimes for ions in MgF_2 are considerably longer than for those in ZBLA. The observed lifetime τ_{ob} is given by the following relation:

$$\frac{1}{\tau_{ob}} = \frac{1}{\tau_R} + \frac{1}{\tau_{NR}} + \frac{1}{\tau_{ET}} . \qquad (5)$$

Here, τ_R represents the radiative lifetime, which is related

to the electric dipole oscillator strength f, by the following equation:[54]

$$f\tau_R = 1.51 \times 10^4 \frac{9}{(n^2+2)^2 n} \lambda^2 , \tag{6}$$

where n is refractive index and λ is the wavelength at the emission peak in meter units. The nonradiative transition rate is τ_{NR} and τ_{ET} is the energy transfer rate.

The emission lifetime of Mn^{2+} at 86 K is 194 ms for MgF_2 and 44 ms for ZBLA. The ratio of the lifetimes is 4.3 which is close to the ratio of the oscillator strengths [4.0 (Table I)]. This result suggests that the change of the lifetime is primarily due to the change of the oscillator strength. This is consistent with the Mn^{2+} emission in $RbMgF_3$ crystals reported by Shinn et al.[64] In $RbMgF_3$ Mn^{2+} ions occupy two sites, one of which has almost octahedral symmetry and the other has C_{3v} symmetry. The emission lifetime from Mn^{2+} in the former site was 150 ms at 15 K, while that from Mn^{2+} in the latter site was only 30 ms. It is also consistent with the difference in the temperature dependence of the emission intensity for Mn^{2+} ions in MgF_2 and ZBLA. As noted earlier the data in Fig. 8 show the intensity increases with temperature for the MgF_2 while the lifetime decreases. This is explained by the splitting of the $^4T_{1g}$ first excited state level (O_h symmetry) into the levels for the D_{2h} symmetry in MgF_2. Thermal promotion of the electrons to the next level results in a broadening of the emission band toward higher energy and an increased intensity due to a change in oscillator strength. Such site symmetry dependence of the emission lifetime of $3d$ ions has been widely investigated in various host lattices.[65] For example, the emission lifetimes of Cr^{3+} ions in noninversion symmetry sites are about a factor of 10 shorter than those in inversion symmetry sites.[66-68] The considerably shorter lifetime of Mn^{2+} emission in ZBLA suggests that in the glass the Mn^{2+} ions are sites with no center of symmetry. On the other hand, the calculated ratio of the ir emission lifetime for Ni^{2+} ions in MgF_2 to that in ZBLA is 35. This value is much higher than the ratio of the oscillator strengths [1.8 (Table I)]. Thus, the lifetime change for Ni^{2+} is not due to a change of the oscillator strength, but to multiphonon transitions or energy transfer. In order to determine which process, samples with different concentration of Ni^{2+} ions were examined. Energy transfer between Ni^{2+} ions in $KZnF_3$ crystal was studied by Ferguson and Masai.[69] They reported very different decay profiles of emission from Ni^{2+} ions at higher concentrations than 0.59%. However, we observed no significant difference in the lifetime of the green emission from ZBLA glass with 1.0 mol % and 0.5 mol % of Ni^{2+} ions. This result suggests that the short lifetimes for Ni^{2+} in ZBLA are primarily caused by the enhanced nonradiative transition processes due to the lack of a center of symmetry. Since the degree of distortion from octahedral ligands is different from site to site, this would result in nonsingle exponential decay as seen in Figs. 6 and 7.

V. CONCLUSION

Comparison of the optical properties of the transition-metal ions Ni^{2+}, Co^{2+}, and Mn^{2+} in ZBLA glass and in MgF_2 crystals shows that the ions in the glass have (1) a much weaker crystal field, (2) higher oscillator strengths, (3) shorter luminescence lifetimes, (4) strong thermal quenching of the luminescence, and (5) different branching ratios for the luminescence.

ACKNOWLEDGMENTS

[1]M. Poulain, J. Non-Cryst. Solids 56, 1 (1983).

[2]D. C. Tran, G. H. Sigel, Jr., and B. Bendow, J. Lightwave Technol. LT-2, 566 (1984).

[3]M. G. Drexhage, in Treatise on Materials Science and Technology, edited by M. Tomozawa and R. H. Doremus (Academice, New York, 1985), Vol. 26, p. 151–243.

[4]S. Shibata, M. Horiguchi, K. Jinguji, S. Mitachi, T. Kanamori, and T. Manabe, Electron. Lett. 17, 775 (1981).

[5]D. C. Tran, K. H. Levin, M. J. Burk, C. F. Fisher, and D. Brower, Proc. SPIE 618, 48 (1986).

[6]For a review up to 1983, see Treatise on Materials Science and Technology, Ref. 3, p. 209.

[7]K. Tanimura, M. D. Shinn, W. A. Sibley, M. G. Drexhage, and R. N. Brown, Phys. Rev. B 30, 2429 (1984).

[8]J. L. Adams and W. A. Sibley, J. Non-Cryst. Solids 76, 267 (1985).

[9]M. Eyal, E. Greenberg, R. Reisfeld, and N. Spector, Chem. Phys. Lett. 117, 108 (1985).

[10]R. Reisfeld, M. Eyal, E. Greenberg, and C. K. Jorgensen, Chem. Phys. Lett. 118, 25 (1985).

[11]Y. Ohishi, S. Mitachi, T. Kanamori, and T. Manabe, Phys. Chem. Glasses 24, 135 (1983).

[12]P. W. France, S. F. Carter, M. W. Moore, and J. R. Williams, Electron. Lett. 21, 602 (1985).

[13]P. W. France, S. F. Carter, and J. M. Parker, Phys. Chem. Glasses 27, 32 (1986).

[14]G. Fonteneau, N. Aliaga, O. Corre, and J. Lucas, Rev. Chim. Miner. 15, 537 (1978).

[15]M. Poulain and J. Lucas, Verres Refract. 32, 505 (1978).

[16]O. Corre, M. Poulain, J. Lucas, and H. Bougault, Verres Refract. 34, 764 (1980).

[17]J. P. Miranday, C. Jacobini, and R. DePape, J. Non-Cryst. Solids 43, 393 (1981).

[18]L. N. Feuerhelm, S. M. Sibley, and W. A. Sibley, J. Solid State Chem. 54, 164 (1984).

[19]R. Reisfeld, Proceedings of the NATO Advanced Research Workshop on Halide Glass for Infrared Fiber Optics, Jilamorna, Portugal, 1986 (unpublished).

[20]Y. Tanabe and S. Sugano, J. Phys. Soc. Jpn. 9, 753 (1954); 9, 766 (1954).

[21]J. Ferguson, H. J. Guggenheim, L. F. Johnson, and H. Kamimura, J. Chem. Phys. 38, 2579 (1963).

[22]J. Ferguson, H. J. Guggenheim, H. Kamimura, and Y. Tanabe, J. Chem. Phys. 42, 775 (1965).

[23]H. M. Gladney, Phys. Rev. 146, 253 (1966).

[24]L. A. Kappers, S. I. Yun, and W. A. Sibley, Phys. Rev. Lett. 29, 943 (1972).

[25]S. I. Yun, L. A. Kappers, and W. A. Sibley, Phys. Rev. B 8, 773 (1973).

[26]W. E. Vehse, K. H. Lee, S. I. Yun, and W. A. Sibley, J. Lumin. 10, 149 (1974).

[27]M. V. Iverson and W. A. Sibley, J. Lumin. 20, 311 (1979).

[28]L. N. Feuerhelm and W. A. Sibley, J. Phys. C 16, 799 (1983).

[29]P. F. Moulton, IEEE J. Quantum. Electron. QE-21, 1582 (1985).

[30]L. F. Johnson, R. E. Dietz, and H. J. Guggenheim, Phys. Rev. Lett. 11, 318 (1963).

[31]L. F. Johnson, R. E. Dietz, and H. J. Guggenheim, Appl. Phys. Lett. 5, 21 (1964).

[32]D. E. McCumber, Phys. Rev. 134, A299 (1964).

[33]L. F. Johnson, H. J. Guggenheim, and R. A. Thomas, Phys. Rev. 149, 179 (1966).

[34]P. F. Moulton, A. Mooradian, and T. B. Reed, Opt. Lett. 3, 164 (1978).

[35]W. H. Baur, Acta Crsytallogr. 9, 515 (1956).

[36]M. G. Drexhage, C. T. Moynihan, M. Saleh Boulos, and K. P. Quinlan, in Proceedings of the Conference on the Physics of Fiber Optics, edited by B. Bendow and S. S. Mitra (American Ceramic Society, Columbus, Ohio, 1981).

[37]C. K. Jorgensen, Absorption Spectra and Chemical Bonding in Complexes (Pergamon, Oxford, 1962).

[38]See, for example, S. Sugano, Y. Tanabe, and H. Kamimura, Multiplets of Transition Metal Ions in Crystals (Academic, New York, 1970).

[39]A. Lecoq and M. Poulain, Verres Refract. 34, 333 (1980).

[40]R. Almeida and J. D. Mackenzie, J. Chem. Phys. 74, 5954 (1981).

[41]I. Yasui and H. Inoue, J. Non-Cryst. Solids 71, 39 (1985).

[42]R. Coupe, D. Louer, J. Lucas, and A. J. Leonard, J. Am. Ceram. Soc. 66, 523 (1983).

[43]See, for example, A. B. P. Leyer, Inorganic Electronic Spectroscopy (Elsevier, New York, 1968).

[44]C. Nelson, T. Furukawa, and W. B. White, Mater. Res. Bull. 18, 959 (1983).

[45]W. B. White and D. S. Knight, Defects in Glasses, Material Research Symposia Proceedings, Boston, 1985, edited by F. L. Galeener, D. L. Griscom, and M. J. Weber (MRS Research Society, Pittsburgh, 1986), Vol. 61, pp. 283—294.

[46]A. Smakula, Z. Phys. 59, 603 (1930).

[47]M. G. Drexhage, O. H. El-Bayoumi, C. T. Moynihan, A. J. Bruce, K. H. Chung, D. L. Gavin, and T. J. Loretz, J. Am. Ceram. Soc. 65, 168 (1982).

[48]A. Duncanson and R. W. H. Stevenson, Proc. Phys. Soc. 72, 1001 (1958).

[49]J. Ferguson, H. U. Gudel, E. R. Krausz, and H. J. Guggenheim, Mol. Phys. 28, 879 (1974); 28, 893 (1974).

[50]J. H. Van Vleck, J. Phys. Chem. 41, 67 (1937).

[51]D. L. Wood, J. Ferguson, K. Knox, and J. F. Dillon, Jr., J. Chem. Phys. 39, 890 (1963).

[52]R. Borromei, G. Ingletto, L. Oleari, and P. Day, J. Chem. Soc. Faraday Trans. 2, 77, 2249 (1981); 78, 1705 (1982).

[53]S. H. Lin, J. Chem. Phys. 44, 3759 (1966).

[54]See, for example, B. DiBartolo, Optical Interaction in Solids (Wiley, New York, 1968).

[55]D. J. Robbins and A. J. Thompson, Mol. Phys. 25, 1103 (1973).

[56]R. Englman and J. Jortner, Mol. Phys. 18, 145 (1970).

[57]L. A. Riseberg and H. W. Moos, Phys. Rev. 174, 429 (1968).

[58]C. B. Layne, W. H. Lowdermilk, and M. J. Weber, Phys. Rev. B 16, 10 (1977).

[59]R. Reisfeld, J. Electrochem. Soc. 131, 1360 (1984).

[60]P. J. Gardner and M. Kasha, J. Chem. Phys. 50, 1543 (1969).

[61]D. J. Robbins and A. J. Thomson, Philos. Mag. 36, 999 (1977).

[62]L. J. Andrews, A. Lempicki, and B. C. McCollum, Chem. Phys. Lett. 74, 404 (1980).

[63]L. J. Andrews, A. Lempicki, and B. C. McCollum, J. Chem. Phys. 74, 5526 (1981).

[64]M. D. Shinn, J. C. Windshief, D. K. Sarder, and W. A. Sibley, Phys. Rev. B 26, 2371 (1982).

[65]P. F. Moulton, in Laser Handbook, edited by M. Bass and M. L. Stitch (Elsevier, New York, 1985), pp. 203—288.

[66]M. J. Weber and T. E. Varitimos, J. Appl. Phys. 45, 810 (1974).

[67]D. F. Nelson and M. D. Sturge, Phys. Rev. 137, A1117 (1965).

[68]J. C. Walling, O. G. Peterson, H. P. Jenssen, R. C. Morris, and E. W. O'Dell, IEEE J. Quantum Electron. QE-16, 1302 (1980).

[69]J. Ferguson and H. Masui, J. Phys. Soc. Jpn. 42, 1640 (1977).